International Journal of
Molecular Sciences

MDPI

Review

Obesity-Related Neuroinflammation: Magnetic Resonance and Microscopy Imaging of the Brain

Anita Woo [1,2,†], Amy Botta [1,2,†], Sammy S. W. Shi [1,2], Tomas Paus [3,4,5,6] and Zdenka Pausova [1,2,6,*]

1 The Hospital for Sick Children, University of Toronto, Toronto, ON M5G 1X8, Canada
2 Departments of Physiology and Nutritional Sciences, University of Toronto, Toronto, ON M5S 1A1, Canada
3 Centre Hospitalier Universitaire Sainte-Justine, University of Montreal, Montreal, QC H3T 1C5, Canada
4 Departments of Psychiatry of Neuroscience, Faculty of Medicine, University of Montreal, Montreal, QC H3T 1J4, Canada
5 Departments of Psychology and Psychiatry, University of Toronto, Toronto, ON M5S 1A1, Canada
6 ECOGENE-21, Chicoutimi, QC G7H 7K9, Canada
* Correspondence: zdenka.pausova@sickkids.ca; Tel.: +1-(416)-813-7654 (ext. 304340); Fax: +1-(416)-813-5771
† These authors contributed equally to this work.

Abstract: Obesity is a major risk factor of Alzheimer's disease and related dementias. The principal feature of dementia is a loss of neurons and brain atrophy. The mechanistic links between obesity and the neurodegenerative processes of dementias are not fully understood, but recent research suggests that obesity-related systemic inflammation and subsequent neuroinflammation may be involved. Adipose tissues release multiple proinflammatory molecules (fatty acids and cytokines) that impact blood and vessel cells, inducing low-grade systemic inflammation that can transition to tissues, including the brain. Inflammation in the brain—neuroinflammation—is one of key elements of the pathobiology of neurodegenerative disorders; it is characterized by the activation of microglia, the resident immune cells in the brain, and by the structural and functional changes of other cells forming the brain parenchyma, including neurons. Such cellular changes have been shown in animal models with direct methods, such as confocal microscopy. In humans, cellular changes are less tangible, as only indirect methods such as magnetic resonance (MR) imaging are usually used. In these studies, obesity and low-grade systemic inflammation have been associated with lower volumes of the cerebral gray matter, cortex, and hippocampus, as well as altered tissue MR properties (suggesting microstructural variations in cellular and molecular composition). How these structural variations in the human brain observed using MR imaging relate to the cellular variations in the animal brain seen with microscopy is not well understood. This review describes the current understanding of neuroinflammation in the context of obesity-induced systemic inflammation, and it highlights need for the bridge between animal microscopy and human MR imaging studies.

Keywords: obesity; neuroinflammation; Alzheimer's disease; magnetic resonance imaging; microscopy

Citation: Woo, A.; Botta, A.; Shi, S.S.W.; Paus, T.; Pausova, Z. Obesity-Related Neuroinflammation: Magnetic Resonance and Microscopy Imaging of the Brain. *Int. J. Mol. Sci.* **2022**, *23*, 8790. https://doi.org/10.3390/ijms23158790

Academic Editor: Javier Conde Aranda

Received: 17 July 2022
Accepted: 6 August 2022
Published: 8 August 2022

1. Introduction

Obesity is a major risk factor of Alzheimer's disease and related dementias (ADRD) [1,2]. It is common, affecting >40% of the adult US population [3], and it increases the risk by 1.6-fold [1,2]; consequently, >13% of the ADRD incidence in the population is attributable to obesity [1,2]. Considering that the prevalence of obesity is still rising [3], this number is expected to increase in the near future. Dementia has a long prodromal phase, developing progressively over decades before the clinical diagnosis [4–6]. An early identification of individuals at risk and the implementation of effective strategies for prevention and early treatment are essential [2], as delaying symptom onset by just 1 year could lower the prevalence of ADRD by >9 million cases in the USA in the next 40 years [2].

The principal feature of dementia is the loss of neurons and brain atrophy [7–9]. The mechanistic links between obesity and the neurodegenerative processes of dementias are

not fully understood, but several lines of evidence suggest that obesity-related systemic inflammation and subsequent neuroinflammation may be involved [10–12]. Adipose tissue adipocytes and macrophages release multiple proinflammatory molecules [13–16] that enter the systemic circulation, where they impact blood cells and endothelial cells lining the vessels, and promote the transition of this low-grade inflammation from the circulation to tissues, including the brain.

Inflammation in the brain—*neuroinflammation*—is one of the key elements of the pathobiology of neurodegenerative disorders [17–19]. On a cellular level, neuroinflammation is characterized by the activation of microglia, resident immune cells in the brain. Microglia alter their structure and function in response to the pro-inflammatory signals from the circulation; other cells forming the brain parenchyma, including astrocytes, oligodendrocytes, and neurons, also alter their structure and function in response to pro-inflammatory signals [20–31]. Collectively, neuroinflammation creates a tissue environment that becomes less neurotrophic and more pro-apoptotic; in the long-term, this may contribute to neurodegeneration. Most of these observations have been made in animal studies using *microscopy imaging*, which has the capacity to examine detailed cellular variations (at 'micrometer' to 'nanometer' resolutions) in (mostly) pre-selected regions of the brain. Such studies are much less feasible in humans, as microscopy imaging is (largely) limited to post mortem samples, which are sparse. In vivo studies of the human brain are mainly conducted with *magnetic resonance (MR) imaging*, which has the capacity to assess volumetric variations of neuroanatomical structures (at 'millimeter' resolution), and variations in tissue MR properties across the whole brain [32]. These human MR imaging studies have shown that adiposity is associated with variations in volumes, as well as in tissue MR-based properties. How these structural variations in the human brain observed with MR imaging relate to the cellular variations in the animal brain seen with microscopy is not well understood. In an attempt to start bridging this gap, here, we will *first* describe the key findings of human studies of the brain in obesity, as assessed with in vivo MR imaging, and *second,* we will describe the main observations in animal studies of the brain in obesity, as examined with ex vivo microscopy imaging. We will begin each part with some basic methodological considerations. We will focus this minireview on the cerebrum, which is the largest part of the brain and which exhibits changes during the preclinical and clinical course of AD (leading ultimately to brain atrophy) [7–9,33]. Note that the hypothalamus is outside the scope of this minireview, as it has been reviewed in the context of obesity previously [34].

2. MR Imaging of the Brain in Obesity

2.1. Methodological Considerations: Basic Principles and Modalities Employed

2.1.1. Basic Principles

MR imaging exploits the magnetization properties of hydrogen nuclei within the imaged tissue, such as the brain. Most often, MR imaging is based on radiofrequency signals generated by hydrogens, which are present in great abundance in biological tissues and have a high gyromagnetic ratio that makes the signal strong. The nucleus of hydrogen consists of one proton. Hydrogen protons are charged particles normally spinning with random orientation. In an MR scanner, a strong (static) magnetic field is present (e.g., 3.0 T), and hydrogen protons become aligned with this magnetic field (i.e., they become magnetized in the longitudinal direction). The direction of magnetization can be changed (or flipped) by an external radio frequency (RF) energy (RF pulse). The angle at which the magnetization is changed (e.g., 90°) or flipped (e.g., 180°) is determined by the duration and strength of the RF pulse. For example, a RF pulse inducing transverse magnetization is when the direction of tissue magnetization is at a 90° angle with respect to the direction of the magnetic field. When the RF pulse is terminated, hydrogen protons return to the original alignment with the magnetic field of the scanner through various relaxation processes, during which they emit RF energy. After a certain period following the initial RF, the emitted signals are measured. Different types of images can be created by different sequences of RF pulses. These sequences are characterized by repetition time (TR), which is the time

between successive RF pulses applied, and time to echo (TE), which is the time between the delivery of the RF pulse and the receipt of the echo signal. The relaxation processes through which excited hydrogen protons realign with the magnetic field of the scanner are characterized by T1- and T2-relaxation times. The T1-relaxation time is the time in which the longitudinal magnetization re-grows (after the RF pulse). The T2-relaxation time is the time in which the transverse magnetization dissipates (after the RF pulse). The relaxation processes differ for hydrogen protons in water molecules in extracellular and intracellular spaces (characterized by higher molecular motion) vs. hydrogen protons in macromolecules in semi-solid cell structures (characterized by lower molecular motion). This phenomenon is key in creating *tissue contrasts on MR images*, visualizing brain structures differing by molecular composition (high content of water (e.g., cerebrospinal fluid) vs. macromolecules (e.g., fatty myelin and lipid composition of cell membranes)).

2.1.2. Modalities Employed

(i) T1-weighted (T1W) imaging uses sequences with short TE and TR, and the signal is mainly determined by the T1-relaxation properties. This imaging modality is commonly used to assess volumes, such as those of the whole brain and its different subregions, including regions the cerebral cortex or the hippocampus (Figure 1). *(ii) T2-weighted (T2W) imaging* uses sequences with longer TE and TR times, and the signal is mainly determined by the T2-relaxation properties; this modality is often used to visualize small lesions in white matter, including white matter hyperintensities, and quantify their volume. *(iii) T2W Fluid Attenuated Inversion Recovery (FLAIR) imaging* uses sequences that are similar to those of T2W imaging, except that the TE and TR times are longer. This modality is also often utilized to visualize and quantify white matter hyperintensities. *(iv) Diffusion tensor imaging (DTI)* is a T2-relaxation time-based imaging technique that assesses the diffusion of water molecules in tissue. It assesses the quantity and directionality of water diffusion within so-called diffusion tensor (conceptualized as a three-dimensional ellipsoid). The diffusion tensor is described using eigenvectors and eigenvalues, with the largest eigenvector being oriented in parallel with neuronal axons. DTI can provide insights into the architecture and integrity of myelinated axons, and the fiber tracts that these axons form. In myelinated axons, water molecules move along the axonal tracts, whereas in axons with disrupted myelin, water molecules can move also radially [35]. The main measures of DTI (characteristics of diffusion tensors) are fractional anisotropy (FA), radial diffusivity (RD), and mean diffusivity (MD). In general, decreased FA, increased RD, and increased MD are considered as indicators of myelin disruption and axonal damage. *(v) Magnetization transfer ratio (MTR) imaging* is also a T2-relaxation time-based modality; it generates contrast on MR images using the process of magnetization transfer between hydrogen protons bound to water and hydrogen protons bound to macromolecules [36–38]. Magnetization transfer is facilitated by the difference in molecular motion between the two pools of hydrogen protons [39]. In white matter, MTR is commonly assumed to index myelin content and structural properties [40], but, especially in gray matter, it may also index variations in lipid content within cell membranes [41,42] or cytosol (e.g., lipid droplets). *(vi) Normalized T1W signal intensity (nT1W-SI)* is a measure derived using the T1W MR imaging technique described above; it is determined as the signal intensity of a brain region of interest normalized by the signal intensity of the whole brain [43]. This metric may also index variations in myelin and lipid content within the cell membranes [41,42] and cytosol (e.g., lipid droplets).

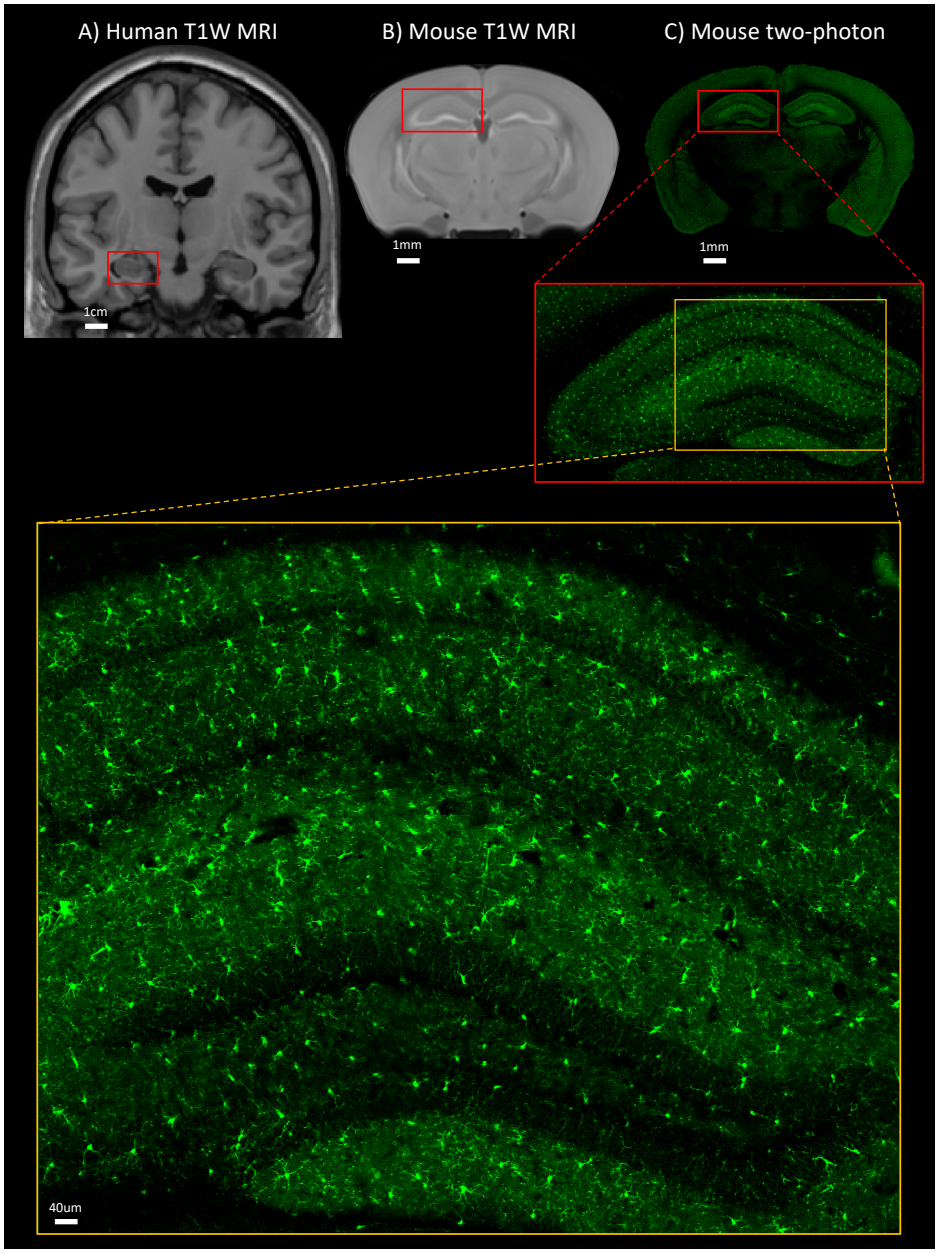

Figure 1. Coronal sections of the brain: (**A**) T1W MR image in humans, (**B**) T1W MRI in mice, and (**C**) two-photon microscopy in microglia-reporter mouse labeled with GFP. Red and yellow rectangles indicate the hippocampus and its subsections. T1W: T1-weighted, MRI: magnetic resonance imaging, GFP: green fluorescent protein. Unpublished data are shown.

2.2. Findings

Before we describe the MR imaging characteristics of the brain in obesity, we will do so for a typical brain.

2.2.1. MR Structure of a Typical Brain

On a neuroanatomical MR image (Figure 1), the cerebrum consists of grey and white matter, with the grey mater including the cerebral cortex, which is a 2 to 4 mm thick outer layer of the cerebrum, and individual subcortical structures, such as the hippocampus [44], and the white matter, which is located underneath the cortex, including structures such as the corpus callosum [44].

2.2.2. MR Structure of the Brain in Obesity

A growing body of research over the last decade has shown that higher body adiposity (and/or systemic inflammation) is associated—mostly cross-sectionally—with variations in brain structure. Much of this research has used body mass index (BMI) as an index of adiposity (body weight in kg/height in m^2), which is an indirect measure of adiposity determined not only by fat mass, but also by muscle and bone mass. Only a few studies have examined body fat more directly (with MRI or computerized tomography), and have quantified the amount of visceral fat (i.e., intra-abdominal fat) [43,45–49]. To assess visceral vs. non-visceral fat (mostly subcutaneous fat, i.e., the fat under the skin) may be important, as visceral fat (vs. subcutaneous fat) produces more proinflammatory molecules [21,50–53], and individuals with a normal BMI but high visceral fat are at higher risk of developing systemic inflammation [50].

The adiposity–brain structure research has been reviewed in detail elsewhere [54]. Here, we highlight only the main findings. Thus, using T1W imaging, most studies have shown that a higher adiposity is associated with a lower brain volume, lower cortical grey volume, and/or lower cortical thickness [45,54–58], and that the associations with cortical thickness are particularly strong in the frontal, temporal, and parietal cortices [54,56]. A higher adiposity is also associated with lower volumes of the hippocampus [57]. Using T2W and T2-FLAIR imaging, a higher adiposity is associated with higher volumes of white matter hyperintensities [59], which are a marker of small vessel disease [59]. Regarding tissue MR properties, several studies have also shown that a higher adiposity is associated with altered white matter properties, as indicated by lower FA and higher MD on DTI [56,60,61], and higher nT1WSI and MTR [43,47,62].

Some of the above studies suggest that the adiposity–brain structure relationships are stronger for visceral fat (accumulating intra-abdominally) than for fat stored elsewhere in the body (mainly subcutaneously) [45,62]. Some studies also suggest that at least a part of the observed adiposity–brain structure relationships may be mediated by systemic inflammation [45,47,62]. Further, it is becoming evident that the adiposity–brain structure relationships do only not exist during adulthood, but also during childhood and adolescence [63], and that they vary across the lifespan [64] and length of exposure (cumulating effects of sustained obesity) [65]. Further, excess adiposity induces not only systemic inflammation, but also metabolic abnormalities, such as insulin resistance and dyslipidemia [66,67], which may potentiate the effects of and/or contribute to the development of neuroinflammation. Thus, e.g., the proinflammatory cytokine TNFα, the production of which is increased by 'obese' adipose tissue, plays a key role in the development of insulin resistance [68], which exists not only in the periphery, but also in the brain [69], where it has been associated with lower cortical thickness in the regions that overlap with those demonstrating a lower thickness in association with higher adiposity [70–76]. Regarding dyslipidemia, a higher adiposity increases the blood concentrations of fatty acids that are enriched in saturated and monounsaturated fatty acids, which can directly stimulate neuroinflammation [67], and that are depleted in polyunsaturated fatty acids, which are essential building blocks of neuronal cell membranes and may inhibit neuroinflammation [77,78]. Consistently, higher blood levels of polyunsaturated fatty acids (incorporated in circulating triacylglycerols) are associated with higher cortical thickness [79]. Finally, many of the observed adiposity–brain structure relationships have been associated with impaired cognitive functioning [80].

Of note, the adiposity–brain structure relationships may exist not only in the direction from obesity to brain structure but also in the direction from brain structure to obesity (via, e.g., the brain regulation of eating behavior [81,82], reviewed recently elsewhere [54]).

In contrast to human research, only a few studies have investigated adiposity–brain structure relationships using brain MR imaging in animal models (Figure 1). Thus, in one mouse study of diet-induced obesity (in response to chronic high-fat diet feeding), a higher adiposity was associated with lower volumes of the frontal, temporal, and parietal

cortices [83]. In another mouse study of diet-induced obesity, a higher adiposity was associated with higher MD on DTI of the cerebrum [84].

3. Microscopy Imaging of the Brain in Obesity

3.1. Methodological Considerations: Basic Principles and Modalities Employed

3.1.1. Basic Principles

Several types of microscopy can be employed to image brain cells and their organelles. Most commonly, these include *optical (light) microscopy* [85], which involves magnifying the image of the object (a tissue sample) by passing light (photons) through it or reflecting light off it, and then examining this light through a single or multiple lens. Less commonly used types of microscopy include *electron microscopy*, which utilizes an electron beam instead of light, and electromagnets instead of traditional lenses; as the electron beam has a far smaller wavelength than light, the image resolution can increase from micrometers to nanometers [86].

Regarding optical microscopy, a variety of methods exist, with fluorescence microscopy being one of the most often used, and it is undergoing, at present, major advancements that are aimed to increase the speed of image acquisition, image resolution, and the volume of imaged tissue. Fluorescence microscopy exploits the capacity of some molecules to fluoresce, that is, to absorb and emit light. For the purpose of microscopy, such fluorescent molecules (probes) can be attached to (or integrated into) different cell structures and imaged. In a confocal microscope, which is the work horse of current fluorescence microcopy, the illumination and detection optics are focused on the same diffraction-limited spot in the sample, which is the only spot imaged by the detector during a confocal scan (while out-of-focus light is rejected), allowing for high-resolution image acquisition in thick tissues [87,88]. To generate a complete image, the spot is moved over the sample, and data are collected point by point (*laser-point scanning*) [87]. Acquiring high-resolution stacks of such images (*optical sectioning*) enables 3D reconstructions of tissue samples [87]. A higher speed of image acquisition is achieved by more recently developed light-sheet fluorescence microscopy [89], which illuminates a thin laminar volume (with a laminar laser beam, termed a light sheet) rather than a single point. A further reduction of out-of-focus light and greater tissue penetration is achieved with two-photon microscopy, which uses two low-energy excitation photons rather than one high-energy excitation photon [90].

These microscope developments have been complemented by substantive innovations in sample preparation, such as *optical tissue clearing* (OTC) [91–93]. OTC methods remove lipids (delipidation), pigments (decolorization), and calcium phosphate (decalcification), and they aim to match the refractive indices of the tissue sample and imaging media, reaching an almost complete level of transparency [91]. This reduces light scattering (and thus optical background) and, as such, allows for the acquisition of high-resolution images of large sections, or even the whole rodent brain [94–96]. Currently, hydrogel-based tissue-clearing methods [94,97–99] are becoming the most commonly used methods. They include 'cleared lipid-extracted acryl-hybridized rigid immunostaining/in situ hybridization-compatible tissue hydrogel' (CLARITY) [100] and 'stabilization to harsh conditions via intramolecular epoxide linkages to prevent degradation' (SHIELD) [101]. CLARITY and SHIELD allow for a uniform delipidation of the tissue, and due to the presence of the hydrogel, also the stabilization and preservation of a large assortment of cell biomolecules through covalent linkages [98]. These preserved tissues can then withstand multiple rounds of antibody staining, stripping, and reprobing, vastly increasing the amount of cellular level information that can be gained from a single sample.

3.1.2. Modalities Employed

Microscopy methods applied to the brain in obesity include: *(i) electron microscopy* for assessing disruption in myelin membranes [29], *(ii) bright-field light microscopy* for evaluating neuronal dendritic spine density [20], *(iii) confocal fluorescence microscopy* for assessing cell-body size and ramifications of microglia [20,28], and *(iv) light-sheet microscopy*

with tissue clearing for examining the blood–brain barrier across the whole brain for uptake of peripherally administered leptin [102].

3.2. Findings

Before we describe observations from microscopy imaging of the brain in obesity, we will describe the cellular composition of the cerebral parenchyma for a typical brain.

3.2.1. Brain Cells in a Typical Brain

The human brain contains approximately 85 billion neurons and about the same number of glial cells [103]. Of the glial cells, ~10% or less are microglia, 19–40% are astrocytes, and 45–75% are oligodendrocytes [104] (Figure 2). *Neurons* are the principal cells of the brain; their degeneration and loss are the primary features of AD and related dementias [105]. A typical neuron consists of a cell body, multiple branching dendrites (dendritic arbor), and a single axon; dendrites have small projections, spines. Axons form a network that totals 176,000 km in length in the adult brain [106]. The speed of conduction along the axon depends on two of its structural properties: axon diameter and myelin sheath. The former is determined by an axonal cytoskeleton constituted by neurofilaments, and the latter insulate axons along their length, except for the nodes of Ranvier, for fast (saltatory) conduction of action potentials [107]. The great majority of axons are short (<3 mm, intra-cortical axons); longer (3–30 mm) and very long (>30 m) axons exit (efferent) and enter (afferent) the cortex, forming the bulk of white matter [108]. Grey matter contains neuronal cell bodies, dendrites, and short axons (and some parts of the longer ones). *Microglia* are the resident immune cells of the brain. They are cells with multiple ramified processes that continuously survey the surrounding parenchyma [109]. When microglia detect cellular debris, apoptotic cells, foreign material, or pro-inflammatory cytokines, they undergo graded 'activation', during which their cell bodies enlarge and their ramified processes shorten [110]. 'Resting' microglia are responsible for scavenging, whereas 'activated' microglia are responsible for cytotoxicity, antigen presentation, and tissue repair. Both resting and activated microglia have the capacity for phagocytosis and extracellular signaling [111]. *Astrocytes* are glial cells with multiple supporting actions. In gray matter, astrocytes have short and thick primary branches that divide into thinner secondary branchlets and tertiary leaflets. The leaflets have characteristic endfeet that encase blood vessels and ensheath thousands of synapses; the processes of a single astrocyte can contact up to 2 million synapses in the human brain [112]. In white matter, astrocytes have long, thin, and mostly unbranched processes [113] that are aligned with axons, mostly at the nodes of Ranvier [114]. Astrocytes support neurons by releasing neurotrophic factors [115]. They also store and supply energy to neurons—they take up glucose to synthesize and store glycogen, which is used later as an energy source when needed [116]. Astrocytes play a major role in the coupling of neuronal activity to blood flow [117–119], and they participate in the formation and elimination of synapses [120]. Astrocytes maintain the fluid and pH homeostasis of the synaptic interstitial fluid via the expression of water channels and ion transporters [121]. *Oligodendrocytes* are glial cells that form myelin sheaths, provide trophic support to neurons, and modulate neuronal excitability [122]. Myelin sheaths are essentially cell membranes of multiple oligodendrocyte processes that are tightly packed (40 or more lipid bilayers) around neuronal axons [123,124]. Myelin sheaths are lipid-rich, containing 70–85% lipids and only 15–30% proteins (which is unlike other cell membranes, which contain approximately equal amounts of lipids and proteins) [125]. The brain parenchyma is separated from the blood circulation by *the blood–brain barrier* (Figure 2), which consists of endothelial cells, pericytes, and astrocytic endfeet. The blood–brain barrier regulates the transport of molecules (and immune cells) to the brain parenchyma [126].

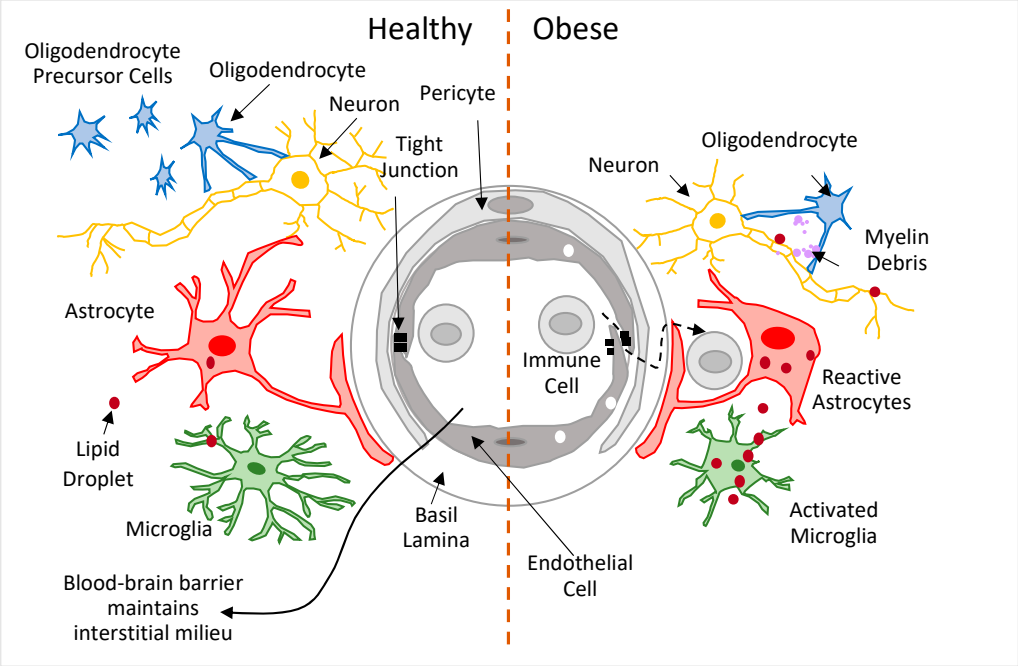

Figure 2. Schematic of cellular composition of brain tissue in healthy and obese brains.

3.2.2. Brain Cells in Obesity

Based mainly on preclinical studies of diet-induced obesity (in mice and rats) in selected brain regions (e.g., parts of the cerebral cortex or hippocampus), obese (vs. lean) animals show neurons with reduced spine density and disrupted myelin, and a higher presence of activated microglia and reactive astrocytes (both with enlarged soma size and reduced ramifications) [20,22,25–31] (Figure 2). These cellular changes may develop due to the release of—by an expanding adipose tissue—multiple pro-inflammatory molecules (saturated and mono-unsaturated FAs and cytokines, such as IL-6 and TNFα) into the circulation, where they generate a hyperlipidemic, pro-inflammatory milieu that disrupts the functional and structural integrity of the blood–brain barrier; consequently, more lipids, proinflammatory molecules, and immune cells enter the brain parenchyma, and promote the development of neuroinflammation [26,27,127,128]—microglia and astrocytes become more proinflammatory (and cytotoxic) and less homeostatic (and neurotrophic). Both microglia and astrocytes increase the production of proinflammatory cytokines and reactive oxygen species, which impair mitochondrial function, damage DNA, proteins, and cell membranes, and promote apoptosis in surrounding cells, including neurons and oligodendrocytes; at the same time, they reduce the phagocytosis of cell and myelin debris and the production of neurotrophic factors that are required for the differentiation of oligodendrocytes and new myelin production, and for neuron survival [129–134]. Finally, in obesity and under inflammatory conditions, microglia, astrocytes, and neurons accumulate lipid droplets (LDs) in their cytoplasm [135,136]. Among others [137–140], LDs sequester excess lipids from the cytoplasm to prevent lipotoxicity, as excess lipids can disrupt the integrity of cell membranes [141]. Reactive oxygen species upregulate lipid synthesis in neurons that transfer excess fatty acids to astrocytes, where they are absorbed by LDs [142,143]. Lipid-laden astrocytes produce proinflammatory factors, such as IL-6 and TNFα [135,136]. Under inflammatory conditions, microglia accumulate LDs [142,144], which are accompanied by compromised phagocytic function. Thus, a number of cellular brain changes have been observed in obesity, but how these changes relate to the observed volumetric and tissue MR properties remains to be elucidated.

4. Conclusions and Future Directions

Human brain MR imaging studies show that a higher body adiposity is associated with lower volumes of the cerebral grey matter (including the cortex and hippocampus) and the alteration of tissue MR properties of the cerebral white matter. Brain MR imaging studies in animals are sparse, but the few that have been conducted provide similar results. Brain microscopy in animal studies shows that diet-induced obesity results in morphological changes of multiple cell types, including microglia, astrocytes, oligodendrocytes, and neurons, but how these cellular changes seen with microscopy relate to the changes in volumes and tissue MR properties observed with MR imaging is not clear at present. Clearly, there is a need for a bridge between animal microscopy and human MR imaging studies. Fast advancing microscopy (with tissue clearing and multiplex immunohistochemistry) that has the capacity to image the entire rodent brain, combined with MR imaging, may provide such a bridge. Towards that end, some novel approaches have been developed to infer cell biology behind the MR imaging data by combining such data with in silico data available in mRNA and protein brain atlases [70,79,145].

Author Contributions: A.W., A.B., S.S.W.S., T.P. and Z.P. researched the literature and wrote the original manuscript. All authors have read and agreed to the published version of the manuscript.

Funding: This review was supported by the National Institutes of Health (R01AG056726).

Conflicts of Interest: The authors declare no commercial or financial relationships that could be construed as a potential conflict of interest.

References

1. Norton, S.; Matthews, F.E.; Barnes, D.E.; Yaffe, K.; Brayne, C. Potential for primary prevention of Alzheimer's disease: An analysis of population-based data. *Lancet Neurol.* **2014**, *13*, 788–794. [CrossRef]
2. Barnes, D.E.; Yaffe, K. The projected effect of risk factor reduction on Alzheimer's disease prevalence. *Lancet Neurol.* **2011**, *10*, 819–828. [CrossRef]
3. Ward, Z.J.; Bleich, S.N.; Cradock, A.L.; Barrett, J.L.; Giles, C.M.; Flax, C.; Long, M.W.; Gortmaker, S.L. Projected U.S. State-Level Prevalence of Adult Obesity and Severe Obesity. *N. Engl. J. Med.* **2019**, *381*, 2440–2450. [CrossRef]
4. Huang, A.R.; Strombotne, K.L.; Horner, E.M.; Lapham, S.J. Adolescent Cognitive Aptitudes and Later-in-Life Alzheimer Disease and Related Disorders. *JAMA Netw. Open* **2018**, *1*, e181726. [CrossRef] [PubMed]
5. Osler, M.; Christensen, G.T.; Garde, E.; Mortensen, E.L.; Christensen, K. Cognitive ability in young adulthood and risk of dementia in a cohort of Danish men, brothers, and twins. *Alzheimer's Dement.* **2017**, *13*, 1355–1363. [CrossRef]
6. Snowdon, D.A.; Kemper, S.J.; Mortimer, J.A.; Greiner, L.H.; Wekstein, D.R.; Markesbery, W.R. Linguistic ability in early life and cognitive function and Alzheimer's disease in late life. Findings from the Nun Study. *JAMA* **1996**, *275*, 528–532. [CrossRef]
7. Pini, L.; Pievani, M.; Bocchetta, M.; Altomare, D.; Bosco, P.; Cavedo, E.; Galluzzi, S.; Marizzoni, M.; Frisoni, G.B. Brain atrophy in Alzheimer's Disease and aging. *Ageing Res. Rev.* **2016**, *30*, 25–48. [CrossRef]
8. Abushakra, S.; Porsteinsson, A.P.; Sabbagh, M.; Bracoud, L.; Schaerer, J.; Power, A.; Hey, J.A.; Scott, D.; Suhy, J.; Tolar, M.; et al. APOE epsilon4/epsilon4 homozygotes with early Alzheimer's disease show accelerated hippocampal atrophy and cortical thinning that correlates with cognitive decline. *Alzheimer's Dement.* **2020**, *6*, e12117. [CrossRef]
9. Young, A.L.; Marinescu, R.V.; Oxtoby, N.P.; Bocchetta, M.; Yong, K.; Firth, N.C.; Cash, D.M.; Thomas, D.L.; Dick, K.M.; Cardoso, J.; et al. Uncovering the heterogeneity and temporal complexity of neurodegenerative diseases with Subtype and Stage Inference. *Nat. Commun.* **2018**, *9*, 4273. [CrossRef]
10. Engelhart, M.J.; Geerlings, M.I.; Meijer, J.; Kiliaan, A.; Ruitenberg, A.; van Swieten, J.C.; Stijnen, T.; Hofman, A.; Witteman, J.C.; Breteler, M.M. Inflammatory proteins in plasma and the risk of dementia: The rotterdam study. *Arch. Neurol.* **2004**, *61*, 668–672. [CrossRef]
11. Schmidt, R.; Schmidt, H.; Curb, J.D.; Masaki, K.; White, L.R.; Launer, L.J. Early inflammation and dementia: A 25-year follow-up of the Honolulu-Asia Aging Study. *Ann. Neurol.* **2002**, *52*, 168–174. [CrossRef] [PubMed]
12. Desikan, R.S.; Schork, A.J.; Wang, Y.; Thompson, W.K.; Dehghan, A.; Ridker, P.M.; Chasman, D.I.; McEvoy, L.K.; Holland, D.; Chen, C.H.; et al. Polygenic Overlap Between C-Reactive Protein, Plasma Lipids, and Alzheimer Disease. *Circulation* **2015**, *131*, 2061–2069. [CrossRef] [PubMed]
13. Visser, M.; Bouter, L.M.; McQuillan, G.M.; Wener, M.H.; Harris, T.B. Elevated C-reactive protein levels in overweight and obese adults. *JAMA* **1999**, *282*, 2131–2135. [CrossRef] [PubMed]
14. Weisberg, S.P.; McCann, D.; Desai, M.; Rosenbaum, M.; Leibel, R.L.; Ferrante, A.W., Jr. Obesity is associated with macrophage accumulation in adipose tissue. *J. Clin. Investig.* **2003**, *112*, 1796–1808. [CrossRef]

15. Trayhurn, P.; Beattie, J.H. Physiological role of adipose tissue: White adipose tissue as an endocrine and secretory organ. *Proc. Nutr. Soc.* **2001**, *60*, 329–339. [CrossRef]
16. Pausova, Z. From big fat cells to high blood pressure: A pathway to obesity-associated hypertension. *Curr. Opin. Nephrol. Hypertens.* **2006**, *15*, 173–178. [CrossRef]
17. Heppner, F.L.; Ransohoff, R.M.; Becher, B. Immune attack: The role of inflammation in Alzheimer disease. *Nat. Rev. Neurosci.* **2015**, *16*, 358–372. [CrossRef]
18. Heneka, M.T.; Carson, M.J.; El Khoury, J.; Landreth, G.E.; Brosseron, F.; Feinstein, D.L.; Jacobs, A.H.; Wyss-Coray, T.; Vitorica, J.; Ransohoff, R.M.; et al. Neuroinflammation in Alzheimer's disease. *Lancet Neurol.* **2015**, *14*, 388–405. [CrossRef]
19. Bellenguez, C.; Kucukali, F.; Jansen, I.E.; Kleineidam, L.; Moreno-Grau, S.; Amin, N.; Naj, A.C.; Campos-Martin, R.; Grenier-Boley, B.; Andrade, V.; et al. New insights into the genetic etiology of Alzheimer's disease and related dementias. *Nat. Genet.* **2022**, *54*, 412–436. [CrossRef]
20. Bocarsly, M.E.; Fasolino, M.; Kane, G.A.; LaMarca, E.A.; Kirschen, G.W.; Karatsoreos, I.N.; McEwen, B.S.; Gould, E. Obesity diminishes synaptic markers, alters microglial morphology, and impairs cognitive function. *Proc. Natl. Acad. Sci. USA* **2015**, *112*, 15731–15736. [CrossRef]
21. Shin, J.A.; Jeong, S.I.; Kim, M.; Yoon, J.C.; Kim, H.S.; Park, E.M. Visceral adipose tissue inflammation is associated with age-related brain changes and ischemic brain damage in aged mice. *Brain Behav. Immun.* **2015**, *50*, 221–231. [CrossRef] [PubMed]
22. Hao, S.; Dey, A.; Yu, X.; Stranahan, A.M. Dietary obesity reversibly induces synaptic stripping by microglia and impairs hippocampal plasticity. *Brain Behav. Immun.* **2016**, *51*, 230–239. [CrossRef] [PubMed]
23. Lecuyer, M.A.; Kebir, H.; Prat, A. Glial influences on BBB functions and molecular players in immune cell trafficking. *Biochim. Biophys. Acta* **2016**, *1862*, 472–482. [CrossRef] [PubMed]
24. Guillemot-Legris, O.; Muccioli, G.G. Obesity-Induced Neuroinflammation: Beyond the Hypothalamus. *Trends Neurosci.* **2017**, *40*, 237–253. [CrossRef] [PubMed]
25. Thompson, J.L.; Drysdale, M.; Baimel, C.; Kaur, M.; MacGowan, T.; Pitman, K.A.; Borgland, S.L. Obesity-Induced Structural and Neuronal Plasticity in the Lateral Orbitofrontal Cortex. *Neuropsychopharmacology* **2017**, *42*, 1480–1490. [CrossRef]
26. Alexaki, V.I. The Impact of Obesity on Microglial Function: Immune, Metabolic and Endocrine Perspectives. *Cells* **2021**, *10*, 1584. [CrossRef]
27. Simpson, D.S.A.; Oliver, P.L. ROS Generation in Microglia: Understanding Oxidative Stress and Inflammation in Neurodegenerative Disease. *Antioxidants* **2020**, *9*, 743. [CrossRef]
28. Reichelt, A.C.; Lemieux, C.A.; Princz-Lebel, O.; Singh, A.; Bussey, T.J.; Saksida, L.M. Age-dependent and region-specific alteration of parvalbumin neurons, perineuronal nets and microglia in the mouse prefrontal cortex and hippocampus following obesogenic diet consumption. *Sci. Rep.* **2021**, *11*, 5593. [CrossRef]
29. Huang, H.T.; Tsai, S.F.; Wu, H.T.; Huang, H.Y.; Hsieh, H.H.; Kuo, Y.M.; Chen, P.S.; Yang, C.S.; Tzeng, S.F. Chronic exposure to high fat diet triggers myelin disruption and interleukin-33 upregulation in hypothalamus. *BMC Neurosci.* **2019**, *20*, 33. [CrossRef]
30. Alkan, I.; Altunkaynak, B.Z.; Gultekin, G.I.; Baycu, C. Hippocampal neural cell loss in high-fat diet-induced obese rats-exploring the protein networks, ultrastructure, biochemical and bioinformatical markers. *J. Chem. Neuroanat.* **2021**, *114*, 101947. [CrossRef]
31. Buckman, L.B.; Hasty, A.H.; Flaherty, D.K.; Buckman, C.T.; Thompson, M.M.; Matlock, B.K.; Weller, K.; Ellacott, K.L. Obesity induced by a high-fat diet is associated with increased immune cell entry into the central nervous system. *Brain Behav. Immun.* **2014**, *35*, 33–42. [CrossRef] [PubMed]
32. Lerch, J.P.; van der Kouwe, A.J.; Raznahan, A.; Paus, T.; Johansen-Berg, H.; Miller, K.L.; Smith, S.M.; Fischl, B.; Sotiropoulos, S.N. Studying neuroanatomy using MRI. *Nat. Neurosci.* **2017**, *20*, 314–326. [CrossRef] [PubMed]
33. Moradi, K.; Faghani, S.; Abdolalizadeh, A.; Khomeijani-Farahani, M.; Ashraf-Ganjouei, A.; Alzheimer's Disease Neuroimaging, I. Biological Features of Reversion from Mild Cognitive Impairment to Normal Cognition: A Study of Cerebrospinal Fluid Markers and Brain Volume. *J. Alzheimer's Dis. Rep.* **2021**, *5*, 179–186. [CrossRef] [PubMed]
34. Jais, A.; Bruning, J.C. Hypothalamic inflammation in obesity and metabolic disease. *J. Clin. Investig.* **2017**, *127*, 24–32. [CrossRef]
35. Aung, W.Y.; Mar, S.; Benzinger, T.L. Diffusion tensor MRI as a biomarker in axonal and myelin damage. *Imaging Med.* **2013**, *5*, 427–440. [CrossRef]
36. Henkelman, R.M.; Stanisz, G.J.; Graham, S.J. Magnetization transfer in MRI: A review. *NMR Biomed.* **2001**, *14*, 57–64. [CrossRef]
37. Sled, J.G. Modelling and interpretation of magnetization transfer imaging in the brain. *NeuroImage* **2018**, *182*, 128–135. [CrossRef]
38. Pike, G.B. Pulsed magnetization transfer contrast in gradient echo imaging: A two-pool analytic description of signal response. *Magn. Reson. Med.* **1996**, *36*, 95–103. [CrossRef]
39. Patel, Y.; Shin, J.; Gowland, P.A.; Pausova, Z.; Paus, T.; consortium, I. Maturation of the Human Cerebral Cortex During Adolescence: Myelin or Dendritic Arbor? *Cereb. Cortex* **2019**, *29*, 3351–3362. [CrossRef]
40. Schmierer, K.; Scaravilli, F.; Altmann, D.R.; Barker, G.J.; Miller, D.H. Magnetization transfer ratio and myelin in postmortem multiple sclerosis brain. *Ann. Neurol.* **2004**, *56*, 407–415. [CrossRef]
41. Fralix, T.A.; Ceckler, T.L.; Wolff, S.D.; Simon, S.A.; Balaban, R.S. Lipid bilayer and water proton magnetization transfer: Effect of cholesterol. *Magn. Reson. Med.* **1991**, *18*, 214–223. [CrossRef] [PubMed]
42. Kucharczyk, W.; Macdonald, P.M.; Stanisz, G.J.; Henkelman, R.M. Relaxivity and magnetization transfer of white matter lipids at MR imaging: Importance of cerebrosides and pH. *Radiology* **1994**, *192*, 521–529. [CrossRef]

43. Schwartz, D.H.; Dickie, E.; Pangelinan, M.M.; Leonard, G.; Perron, M.; Pike, G.B.; Richer, L.; Veillette, S.; Pausova, Z.; Paus, T. Adiposity is associated with structural properties of the adolescent brain. *NeuroImage* **2014**, *103*, 192–201. [CrossRef] [PubMed]
44. Fields, R.D. Neuroscience. Change in the brain's white matter. *Science* **2010**, *330*, 768–769. [CrossRef] [PubMed]
45. Debette, S.; Beiser, A.; Hoffmann, U.; Decarli, C.; O'Donnell, C.J.; Massaro, J.M.; Au, R.; Himali, J.J.; Wolf, P.A.; Fox, C.S.; et al. Visceral fat is associated with lower brain volume in healthy middle-aged adults. *Ann. Neurol.* **2010**, *68*, 136–144. [CrossRef]
46. Syme, C.; Abrahamowicz, M.; Leonard, G.T.; Perron, M.; Pitiot, A.; Qiu, X.; Richer, L.; Totman, J.; Veillette, S.; Xiao, Y.; et al. Intra-abdominal adiposity and individual components of the metabolic syndrome in adolescence: Sex differences and underlying mechanisms. *Arch. Pediatr. Adolesc. Med.* **2008**, *162*, 453–461. [CrossRef]
47. Sliz, E.; Shin, J.; Syme, C.; Patel, Y.; Parker, N.; Richer, L.; Gaudet, D.; Bennett, S.; Paus, T.; Pausova, Z. A variant near DHCR24 associates with microstructural properties of white matter and peripheral lipid metabolism in adolescents. *Mol. Psychiatry* **2021**, *26*, 3795–3805. [CrossRef]
48. Kim, K.W.; Seo, H.; Kwak, M.S.; Kim, D. Visceral obesity is associated with white matter hyperintensity and lacunar infarct. *Int. J. Obes.* **2017**, *41*, 683–688. [CrossRef] [PubMed]
49. Higuchi, S.; Kabeya, Y.; Kato, K. Visceral-to-subcutaneous fat ratio is independently related to small and large cerebrovascular lesions even in healthy subjects. *Atherosclerosis* **2017**, *259*, 41–45. [CrossRef]
50. Pou, K.M.; Massaro, J.M.; Hoffmann, U.; Vasan, R.S.; Maurovich-Horvat, P.; Larson, M.G.; Keaney, J.F., Jr.; Meigs, J.B.; Lipinska, I.; Kathiresan, S.; et al. Visceral and subcutaneous adipose tissue volumes are cross-sectionally related to markers of inflammation and oxidative stress: The Framingham Heart Study. *Circulation* **2007**, *116*, 1234–1241. [CrossRef]
51. Tchernof, A.; Despres, J.P. Pathophysiology of human visceral obesity: An update. *Physiol. Rev.* **2013**, *93*, 359–404. [CrossRef] [PubMed]
52. Hocking, S.L.; Stewart, R.L.; Brandon, A.E.; Suryana, E.; Stuart, E.; Baldwin, E.M.; Kolumam, G.A.; Modrusan, Z.; Junutula, J.R.; Gunton, J.E.; et al. Subcutaneous fat transplantation alleviates diet-induced glucose intolerance and inflammation in mice. *Diabetologia* **2015**, *58*, 1587–1600. [CrossRef] [PubMed]
53. Klein, S.; Fontana, L.; Young, V.L.; Coggan, A.R.; Kilo, C.; Patterson, B.W.; Mohammed, B.S. Absence of an effect of liposuction on insulin action and risk factors for coronary heart disease. *N. Engl. J. Med.* **2004**, *350*, 2549–2557. [CrossRef]
54. Garcia-Garcia, I.; Michaud, A.; Jurado, M.A.; Dagher, A.; Morys, F. Mechanisms linking obesity and its metabolic comorbidities with cerebral grey and white matter changes. *Rev. Endocr. Metab. Disord.* **2022**, *23*, 833–843. [CrossRef]
55. Hamer, M.; Batty, G.D. Association of body mass index and waist-to-hip ratio with brain structure: UK Biobank study. *Neurology* **2019**, *92*, e594–e600. [CrossRef] [PubMed]
56. Cox, S.R.; Lyall, D.M.; Ritchie, S.J.; Bastin, M.E.; Harris, M.A.; Buchanan, C.R.; Fawns-Ritchie, C.; Barbu, M.C.; de Nooij, L.; Reus, L.M.; et al. Associations between vascular risk factors and brain MRI indices in UK Biobank. *Eur. Heart J.* **2019**, *40*, 2290–2300. [CrossRef]
57. Gurholt, T.P.; Kaufmann, T.; Frei, O.; Alnaes, D.; Haukvik, U.K.; van der Meer, D.; Moberget, T.; O'Connell, K.S.; Leinhard, O.D.; Linge, J.; et al. Population-based body-brain mapping links brain morphology with anthropometrics and body composition. *Transl. Psychiatry* **2021**, *11*, 295. [CrossRef]
58. Debette, S.; Seshadri, S.; Beiser, A.; Au, R.; Himali, J.J.; Palumbo, C.; Wolf, P.A.; DeCarli, C. Midlife vascular risk factor exposure accelerates structural brain aging and cognitive decline. *Neurology* **2011**, *77*, 461–468. [CrossRef]
59. Wardlaw, J.M.; Smith, C.; Dichgans, M. Small vessel disease: Mechanisms and clinical implications. *Lancet Neurol.* **2019**, *18*, 684–696. [CrossRef]
60. Zhang, R.; Beyer, F.; Lampe, L.; Luck, T.; Riedel-Heller, S.G.; Loeffler, M.; Schroeter, M.L.; Stumvoll, M.; Villringer, A.; Witte, A.V. White matter microstructural variability mediates the relation between obesity and cognition in healthy adults. *NeuroImage* **2018**, *172*, 239–249. [CrossRef]
61. Daoust, J.; Schaffer, J.; Zeighami, Y.; Dagher, A.; Garcia-Garcia, I.; Michaud, A. White matter integrity differences in obesity: A meta-analysis of diffusion tensor imaging studies. *Neurosci. Biobehav. Rev.* **2021**, *129*, 133–141. [CrossRef] [PubMed]
62. Syme, C.; Pelletier, S.; Shin, J.; Abrahamowicz, M.; Leonard, G.; Perron, M.; Richer, L.; Veillette, S.; Gaudet, D.; Pike, B.; et al. Visceral fat-related systemic inflammation and the adolescent brain: A mediating role of circulating glycerophosphocholines. *Int. J. Obes.* **2019**, *43*, 1223–1230. [CrossRef] [PubMed]
63. Melka, M.G.; Gillis, J.; Bernard, M.; Abrahamowicz, M.; Chakravarty, M.M.; Leonard, G.T.; Perron, M.; Richer, L.; Veillette, S.; Banaschewski, T.; et al. FTO, obesity and the adolescent brain. *Hum. Mol. Genet.* **2013**, *22*, 1050–1058. [CrossRef]
64. Shaw, M.E.; Sachdev, P.S.; Abhayaratna, W.; Anstey, K.J.; Cherbuin, N. Body mass index is associated with cortical thinning with different patterns in mid- and late-life. *Int. J. Obes.* **2018**, *42*, 455–461. [CrossRef] [PubMed]
65. Norris, T.; Cole, T.J.; Bann, D.; Hamer, M.; Hardy, R.; Li, L.; Ong, K.K.; Ploubidis, G.B.; Viner, R.; Johnson, W. Duration of obesity exposure between ages 10 and 40 years and its relationship with cardiometabolic disease risk factors: A cohort study. *PLoS Med.* **2020**, *17*, e1003387. [CrossRef] [PubMed]
66. Czech, M.P. Insulin action and resistance in obesity and type 2 diabetes. *Nat. Med.* **2017**, *23*, 804–814. [CrossRef] [PubMed]
67. Raheem, J.; Sliz, E.; Shin, J.; Holmes, M.V.; Pike, G.B.; Richer, L.; Gaudet, D.; Paus, T.; Pausova, Z. Visceral adiposity is associated with metabolic profiles predictive of type 2 diabetes and myocardial infarction. *Commun. Med.* **2022**, *2*, 81. [CrossRef]
68. Hotamisligil, G.S.; Arner, P.; Caro, J.F.; Atkinson, R.L.; Spiegelman, B.M. Increased adipose tissue expression of tumor necrosis factor-alpha in human obesity and insulin resistance. *J. Clin. Investig.* **1995**, *95*, 2409–2415. [CrossRef]

69. Arnold, S.E.; Arvanitakis, Z.; Macauley-Rambach, S.L.; Koenig, A.M.; Wang, H.Y.; Ahima, R.S.; Craft, S.; Gandy, S.; Buettner, C.; Stoeckel, L.E.; et al. Brain insulin resistance in type 2 diabetes and Alzheimer disease: Concepts and conundrums. *Nat. Rev. Neurol.* **2018**, *14*, 168–181. [CrossRef]
70. Shin, J.; Pelletier, S.; Richer, L.; Pike, G.B.; Gaudet, D.; Paus, T.; Pausova, Z. Adiposity-related insulin resistance and thickness of the cerebral cortex in middle-aged adults. *J. Neuroendocrinol.* **2020**, *32*, e12921. [CrossRef]
71. Brundel, M.; van den Heuvel, M.; de Bresser, J.; Kappelle, L.J.; Biessels, G.J.; Utrecht Diabetic Encephalopathy Study, G. Cerebral cortical thickness in patients with type 2 diabetes. *J. Neurol. Sci.* **2010**, *299*, 126–130. [CrossRef] [PubMed]
72. Chen, Z.; Sun, J.; Yang, Y.; Lou, X.; Wang, Y.; Wang, Y.; Ma, L. Cortical thinning in type 2 diabetes mellitus and recovering effects of insulin therapy. *J. Clin. Neurosci.* **2015**, *22*, 275–279. [CrossRef] [PubMed]
73. van Velsen, E.F.; Vernooij, M.W.; Vrooman, H.A.; van der Lugt, A.; Breteler, M.M.; Hofman, A.; Niessen, W.J.; Ikram, M.A. Brain cortical thickness in the general elderly population: The Rotterdam Scan Study. *Neurosci. Lett.* **2013**, *550*, 189–194. [CrossRef] [PubMed]
74. Lu, R.; Aziz, N.A.; Diers, K.; Stocker, T.; Reuter, M.; Breteler, M.M.B. Insulin resistance accounts for metabolic syndrome-related alterations in brain structure. *Hum. Brain Mapp.* **2021**, *42*, 2434–2444. [CrossRef]
75. Baker, L.D.; Cross, D.J.; Minoshima, S.; Belongia, D.; Watson, G.S.; Craft, S. Insulin resistance and Alzheimer-like reductions in regional cerebral glucose metabolism for cognitively normal adults with prediabetes or early type 2 diabetes. *Arch. Neurol.* **2011**, *68*, 51–57. [CrossRef]
76. Willette, A.A.; Bendlin, B.B.; Starks, E.J.; Birdsill, A.C.; Johnson, S.C.; Christian, B.T.; Okonkwo, O.C.; La Rue, A.; Hermann, B.P.; Koscik, R.L.; et al. Association of Insulin Resistance with Cerebral Glucose Uptake in Late Middle-Aged Adults at Risk for Alzheimer Disease. *JAMA Neurol.* **2015**, *72*, 1013–1020. [CrossRef]
77. Bazinet, R.P.; Laye, S. Polyunsaturated fatty acids and their metabolites in brain function and disease. *Nat. Rev. Neurosci.* **2014**, *15*, 771–785. [CrossRef]
78. Rapoport, S.I.; Chang, M.C.; Spector, A.A. Delivery and turnover of plasma-derived essential PUFAs in mammalian brain. *J. Lipid Res.* **2001**, *42*, 678–685. [CrossRef]
79. Sliz, E.; Shin, J.; Syme, C.; Black, S.; Seshadri, S.; Paus, T.; Pausova, Z. Thickness of the cerebral cortex shows positive association with blood levels of triacylglycerols carrying 18-carbon fatty acids. *Commun. Biol.* **2020**, *3*, 456. [CrossRef]
80. Nguyen, J.C.; Killcross, A.S.; Jenkins, T.A. Obesity and cognitive decline: Role of inflammation and vascular changes. *Front. Neurosci.* **2014**, *8*, 375. [CrossRef]
81. Haghighi, A.; Schwartz, D.H.; Abrahamowicz, M.; Leonard, G.T.; Perron, M.; Richer, L.; Veillette, S.; Gaudet, D.; Paus, T.; Pausova, Z. Prenatal exposure to maternal cigarette smoking, amygdala volume, and fat intake in adolescence. *JAMA Psychiatry* **2013**, *70*, 98–105. [CrossRef] [PubMed]
82. Haghighi, A.; Melka, M.G.; Bernard, M.; Abrahamowicz, M.; Leonard, G.T.; Richer, L.; Perron, M.; Veillette, S.; Xu, C.J.; Greenwood, C.M.; et al. Opioid receptor mu 1 gene, fat intake and obesity in adolescence. *Mol. Psychiatry* **2014**, *19*, 63–68. [CrossRef]
83. Rollins, C.P.E.; Gallino, D.; Kong, V.; Ayranci, G.; Devenyi, G.A.; Germann, J.; Chakravarty, M.M. Contributions of a high-fat diet to Alzheimer's disease-related decline: A longitudinal behavioural and structural neuroimaging study in mouse models. *NeuroImage Clin.* **2019**, *21*, 101606. [CrossRef]
84. Guadilla, I.; Lizarbe, B.; Barrios, L.; Cerdán, S.; López-Larrubia, P. Integrative analysis of physiological responses to high fat feeding with diffusion tensor images and neurochemical profiles of the mouse brain. *Int. J. Obes.* **2021**, *45*, 1203–1214. [CrossRef] [PubMed]
85. Osten, P.; Margrie, T.W. Mapping brain circuitry with a light microscope. *Nat. Methods* **2013**, *10*, 515–523. [CrossRef] [PubMed]
86. Nahirney, P.C.; Tremblay, M.E. Brain Ultrastructure: Putting the Pieces Together. *Front. Cell Dev. Biol.* **2021**, *9*, 629503. [CrossRef]
87. Elliott, A.D. Confocal Microscopy: Principles and Modern Practices. *Curr. Protoc. Cytom.* **2020**, *92*, e68. [CrossRef]
88. Paddock, S.W. Principles and practices of laser scanning confocal microscopy. *Mol. Biotechnol.* **2000**, *16*, 127–149. [CrossRef]
89. Hillman, E.M.C.; Voleti, V.; Li, W.; Yu, H. Light-Sheet Microscopy in Neuroscience. *Annu. Rev. Neurosci.* **2019**, *42*, 295–313. [CrossRef]
90. Svoboda, K.; Yasuda, R. Principles of two-photon excitation microscopy and its applications to neuroscience. *Neuron* **2006**, *50*, 823–839. [CrossRef]
91. Ueda, H.R.; Ertürk, A.; Chung, K.; Gradinaru, V.; Chédotal, A.; Tomancak, P.; Keller, P.J. Tissue clearing and its applications in neuroscience. *Nat. Rev. Neurosci.* **2020**, *21*, 61–79. [CrossRef] [PubMed]
92. Liang, X.; Luo, H. Optical Tissue Clearing: Illuminating Brain Function and Dysfunction. *Theranostics* **2021**, *11*, 3035–3051. [CrossRef] [PubMed]
93. Parra-Damas, A.; Saura, C.A. Tissue Clearing and Expansion Methods for Imaging Brain Pathology in Neurodegeneration: From Circuits to Synapses and Beyond. *Front. Neurosci.* **2020**, *14*, 914. [CrossRef]
94. Tainaka, K.; Kuno, A.; Kubota, S.I.; Murakami, T.; Ueda, H.R. Chemical Principles in Tissue Clearing and Staining Protocols for Whole-Body Cell Profiling. *Annu. Rev. Cell Dev. Biol.* **2016**, *32*, 713–741. [CrossRef] [PubMed]
95. Ueda, H.R.; Dodt, H.-U.; Osten, P.; Economo, M.N.; Chandrashekar, J.; Keller, P.J. Whole-brain profiling of cells and circuits in mammals by tissue clearing and light-sheet microscopy. *Neuron* **2020**, *106*, 369–387. [CrossRef] [PubMed]

96. Cai, R.; Pan, C.; Ghasemigharagoz, A.; Todorov, M.I.; Förstera, B.; Zhao, S.; Bhatia, H.S.; Parra-Damas, A.; Mrowka, L.; Theodorou, D. Panoptic imaging of transparent mice reveals whole-body neuronal projections and skull–meninges connections. *Nat. Neurosci.* **2019**, *22*, 317–327. [CrossRef]
97. Hofmann, J.; Keppler, S.J. Tissue clearing and 3D imaging—Putting immune cells into context. *J. Cell Sci.* **2021**, *134*, jcs258494. [CrossRef]
98. Richardson, D.S.; Guan, W.; Matsumoto, K.; Pan, C.; Chung, K.; Ertürk, A.; Ueda, H.R.; Lichtman, J.W. Tissue Clearing. *Nat. Rev. Methods Prim.* **2021**, *1*, 84. [CrossRef]
99. Gómez-Gaviro, M.V.; Sanderson, D.; Ripoll, J.; Desco, M. Biomedical Applications of Tissue Clearing and Three-Dimensional Imaging in Health and Disease. *iScience* **2020**, *23*, 101432. [CrossRef]
100. Guo, Z.; Zheng, Y.; Zhang, Y. CLARITY techniques based tissue clearing: Types and differences. *Folia Morphol.* **2022**, *81*, 1–12. [CrossRef]
101. Park, Y.-G.; Sohn, C.H.; Chen, R.; McCue, M.; Yun, D.H.; Drummond, G.T.; Ku, T.; Evans, N.B.; Oak, H.C.; Trieu, W. Protection of tissue physicochemical properties using polyfunctional crosslinkers. *Nat. Biotechnol.* **2019**, *37*, 73–83. [CrossRef]
102. Harrison, L.; Schriever, S.C.; Feuchtinger, A.; Kyriakou, E.; Baumann, P.; Pfuhlmann, K.; Messias, A.C.; Walch, A.; Tschop, M.H.; Pfluger, P.T. Fluorescent blood-brain barrier tracing shows intact leptin transport in obese mice. *Int. J. Obes.* **2019**, *43*, 1305–1318. [CrossRef] [PubMed]
103. von Bartheld, C.S.; Bahney, J.; Herculano-Houzel, S. The search for true numbers of neurons and glial cells in the human brain: A review of 150 years of cell counting. *J. Comp. Neurol.* **2016**, *524*, 3865–3895. [CrossRef] [PubMed]
104. Pelvig, D.P.; Pakkenberg, H.; Stark, A.K.; Pakkenberg, B. Neocortical glial cell numbers in human brains. *Neurobiol. Aging* **2008**, *29*, 1754–1762. [CrossRef]
105. Alzheimer, A.; Stelzmann, R.A.; Schnitzlein, H.N.; Murtagh, F.R. An English translation of Alzheimer's 1907 paper, "Uber eine eigenartige Erkankung der Hirnrinde". *Clin. Anat.* **1995**, *8*, 429–431. [CrossRef] [PubMed]
106. Marner, L.; Pakkenberg, B. Total length of nerve fibers in prefrontal and global white matter of chronic schizophrenics. *J. Psychiatr. Res.* **2003**, *37*, 539–547. [CrossRef]
107. Paus, T. Growth of white matter in the adolescent brain: Myelin or axon? *Brain Cogn.* **2010**, *72*, 26–35. [CrossRef] [PubMed]
108. Schüz, A.; Braitenberg, V. *The Human Cortical White Matter: Quantitative Aspects of Cortico-Cortical Long-Range Connectivity*; Taylor & Francis: London, UK; New York, NY, USA, 2002.
109. Nimmerjahn, A.; Kirchhoff, F.; Helmchen, F. Resting microglial cells are highly dynamic surveillants of brain parenchyma in vivo. *Science* **2005**, *308*, 1314–1318. [CrossRef]
110. Fernandez-Arjona, M.D.M.; Grondona, J.M.; Granados-Duran, P.; Fernandez-Llebrez, P.; Lopez-Avalos, M.D. Microglia Morphological Categorization in a Rat Model of Neuroinflammation by Hierarchical Cluster and Principal Components Analysis. *Front. Cell. Neurosci.* **2017**, *11*, 235. [CrossRef]
111. Arcuri, C.; Mecca, C.; Bianchi, R.; Giambanco, I.; Donato, R. The Pathophysiological Role of Microglia in Dynamic Surveillance, Phagocytosis and Structural Remodeling of the Developing CNS. *Front. Mol. Neurosci.* **2017**, *10*, 191. [CrossRef]
112. Liddelow, S.; Barres, B. SnapShot: Astrocytes in Health and Disease. *Cell* **2015**, *162*, 1170–1170.e1. [CrossRef] [PubMed]
113. Tabata, H. Diverse subtypes of astrocytes and their development during corticogenesis. *Front. Neurosci.* **2015**, *9*, 114. [CrossRef] [PubMed]
114. Kohler, S.; Winkler, U.; Hirrlinger, J. Heterogeneity of Astrocytes in Grey and White Matter. *Neurochem. Res.* **2021**, *46*, 3–14. [CrossRef] [PubMed]
115. Miranda, M.; Morici, J.F.; Zanoni, M.B.; Bekinschtein, P. Brain-Derived Neurotrophic Factor: A Key Molecule for Memory in the Healthy and the Pathological Brain. *Front. Cell. Neurosci.* **2019**, *13*, 363. [CrossRef] [PubMed]
116. Mason, S. Lactate Shuttles in Neuroenergetics-Homeostasis, Allostasis and Beyond. *Front. Neurosci.* **2017**, *11*, 43. [CrossRef]
117. Murat, C.B.; Garcia-Caceres, C. Astrocyte Gliotransmission in the Regulation of Systemic Metabolism. *Metabolites* **2021**, *11*, 732. [CrossRef]
118. Fujii, Y.; Maekawa, S.; Morita, M. Astrocyte calcium waves propagate proximally by gap junction and distally by extracellular diffusion of ATP released from volume-regulated anion channels. *Sci. Rep.* **2017**, *7*, 13115. [CrossRef]
119. Filosa, J.A.; Morrison, H.W.; Iddings, J.A.; Du, W.; Kim, K.J. Beyond neurovascular coupling, role of astrocytes in the regulation of vascular tone. *Neuroscience* **2016**, *323*, 96–109. [CrossRef]
120. Chung, W.S.; Allen, N.J.; Eroglu, C. Astrocytes Control Synapse Formation, Function, and Elimination. *Cold Spring Harb. Perspect. Biol.* **2015**, *7*, a020370. [CrossRef]
121. Sofroniew, M.V.; Vinters, H.V. Astrocytes: Biology and pathology. *Acta Neuropathol.* **2010**, *119*, 7–35. [CrossRef]
122. Philips, T.; Rothstein, J.D. Oligodendroglia: Metabolic supporters of neurons. *J. Clin. Investig.* **2017**, *127*, 3271–3280. [CrossRef] [PubMed]
123. Poitelon, Y.; Kopec, A.M.; Belin, S. Myelin Fat Facts: An Overview of Lipids and Fatty Acid Metabolism. *Cells* **2020**, *9*, 812. [CrossRef] [PubMed]
124. Salzer, J.L. Schwann cell myelination. *Cold Spring Harb. Perspect. Biol.* **2015**, *7*, a020529. [CrossRef]
125. Ozgen, H.; Baron, W.; Hoekstra, D.; Kahya, N. Oligodendroglial membrane dynamics in relation to myelin biogenesis. *Cell. Mol. Life Sci.* **2016**, *73*, 3291–3310. [CrossRef] [PubMed]

126. Abbott, N.J.; Patabendige, A.A.; Dolman, D.E.; Yusof, S.R.; Begley, D.J. Structure and function of the blood-brain barrier. *Neurobiol. Dis.* **2010**, *37*, 13–25. [CrossRef] [PubMed]
127. Farooqui, A.A.; Horrocks, L.A.; Farooqui, T. Modulation of inflammation in brain: A matter of fat. *J. Neurochem.* **2007**, *101*, 577–599. [CrossRef]
128. Rudge, J.D. A New Hypothesis for Alzheimer's Disease: The Lipid Invasion Model. *J. Alzheimer's Dis. Rep.* **2022**, *6*, 129–161. [CrossRef]
129. Leyrolle, Q.; Layé, S.; Nadjar, A. Direct and indirect effects of lipids on microglia function. *Neurosci. Lett.* **2019**, *708*, 134348. [CrossRef]
130. Butler, M.J.; Cole, R.M.; Deems, N.P.; Belury, M.A.; Barrientos, R.M. Fatty food, fatty acids, and microglial priming in the adult and aged hippocampus and amygdala. *Brain Behav. Immun.* **2020**, *89*, 145–158. [CrossRef]
131. Tognatta, R.; Karl, M.T.; Fyffe-Maricich, S.L.; Popratiloff, A.; Garrison, E.D.; Schenck, J.K.; Abu-Rub, M.; Miller, R.H. Astrocytes Are Required for Oligodendrocyte Survival and Maintenance of Myelin Compaction and Integrity. *Front. Cell. Neurosci.* **2020**, *14*, 74. [CrossRef]
132. Liddelow, S.A.; Guttenplan, K.A.; Clarke, L.E.; Bennett, F.C.; Bohlen, C.J.; Schirmer, L.; Bennett, M.L.; Munch, A.E.; Chung, W.S.; Peterson, T.C.; et al. Neurotoxic reactive astrocytes are induced by activated microglia. *Nature* **2017**, *541*, 481–487. [CrossRef] [PubMed]
133. Miron, V.E.; Boyd, A.; Zhao, J.W.; Yuen, T.J.; Ruckh, J.M.; Shadrach, J.L.; van Wijngaarden, P.; Wagers, A.J.; Williams, A.; Franklin, R.J.; et al. M2 microglia and macrophages drive oligodendrocyte differentiation during CNS remyelination. *Nat. Neurosci.* **2013**, *16*, 1211–1218. [CrossRef] [PubMed]
134. Kotter, M.R.; Li, W.W.; Zhao, C.; Franklin, R.J. Myelin impairs CNS remyelination by inhibiting oligodendrocyte precursor cell differentiation. *J. Neurosci.* **2006**, *26*, 328–332. [CrossRef] [PubMed]
135. Rahman, M.H.; Kim, M.S.; Lee, I.K.; Yu, R.; Suk, K. Interglial Crosstalk in Obesity-Induced Hypothalamic Inflammation. *Front. Neurosci.* **2018**, *12*, 939. [CrossRef]
136. Kwon, Y.H.; Kim, J.; Kim, C.S.; Tu, T.H.; Kim, M.S.; Suk, K.; Kim, D.H.; Lee, B.J.; Choi, H.S.; Park, T.; et al. Hypothalamic lipid-laden astrocytes induce microglia migration and activation. *FEBS Lett.* **2017**, *591*, 1742–1751. [CrossRef]
137. Bozza, P.T.; Viola, J.P. Lipid droplets in inflammation and cancer. *Prostaglandins Leukot. Essent. Fat. Acids* **2010**, *82*, 243–250. [CrossRef]
138. Yaqoob, P. Fatty acids as gatekeepers of immune cell regulation. *Trends Immunol.* **2003**, *24*, 639–645. [CrossRef]
139. Unger, R.H.; Clark, G.O.; Scherer, P.E.; Orci, L. Lipid homeostasis, lipotoxicity and the metabolic syndrome. *Biochim. Biophys. Acta* **2010**, *1801*, 209–214. [CrossRef]
140. Rambold, A.S.; Cohen, S.; Lippincott-Schwartz, J. Fatty acid trafficking in starved cells: Regulation by lipid droplet lipolysis, autophagy, and mitochondrial fusion dynamics. *Dev. Cell* **2015**, *32*, 678–692. [CrossRef]
141. Loving, B.A.; Bruce, K.D. Lipid and Lipoprotein Metabolism in Microglia. *Front. Physiol.* **2020**, *11*, 393. [CrossRef]
142. Liu, L.; MacKenzie, K.R.; Putluri, N.; Maletić-Savatić, M.; Bellen, H.J. The Glia-Neuron Lactate Shuttle and Elevated ROS Promote Lipid Synthesis in Neurons and Lipid Droplet Accumulation in Glia via APOE/D. *Cell Metab.* **2017**, *26*, 719–737.e716. [CrossRef] [PubMed]
143. Smolič, T.; Tavčar, P.; Horvat, A.; Černe, U.; Halužan Vasle, A.; Tratnjek, L.; Kreft, M.E.; Scholz, N.; Matis, M.; Petan, T. Astrocytes in stress accumulate lipid droplets. *Glia* **2021**, *69*, 1540–1562. [CrossRef] [PubMed]
144. Marschallinger, J.; Iram, T.; Zardeneta, M.; Lee, S.E.; Lehallier, B.; Haney, M.S.; Pluvinage, J.V.; Mathur, V.; Hahn, O.; Morgens, D.W.; et al. Lipid-droplet-accumulating microglia represent a dysfunctional and proinflammatory state in the aging brain. *Nat. Neurosci.* **2020**, *23*, 194–208. [CrossRef] [PubMed]
145. Shin, J.; French, L.; Xu, T.; Leonard, G.; Perron, M.; Pike, G.B.; Richer, L.; Veillette, S.; Pausova, Z.; Paus, T. Cell-Specific Gene-Expression Profiles and Cortical Thickness in the Human Brain. *Cereb. Cortex* **2018**, *28*, 3267–3277. [CrossRef] [PubMed]